ResearchGate

See discussions, stats, and author profiles for this publication at: https://www.researchgate.net/publication/257665806

Co-crystal/salt crystal structure disorder of trichloroacetic acid–N-methylurea complex with double system of homo- and heteronuclear O–H···O/N–H···O hydrogen bonds: X-ray investig...

ARTICLE *in* STRUCTURAL CHEMISTRY · DECEMBER 2012

Impact Factor: 1.84 · DOI: 10.1007/s11224-012-9980-7

CITATIONS
5

READS
36

1 AUTHOR:

Agnieszka J. Rybarczyk-Pirek
University of Lodz
47 PUBLICATIONS **330** CITATIONS

SEE PROFILE

Available from: Agnieszka J. Rybarczyk-Pirek
Retrieved on: 23 January 2016

Struct Chem (2012) 23:1739–1749
DOI 10.1007/s11224-012-9980-7

ORIGINAL RESEARCH

Co-crystal/salt crystal structure disorder of trichloroacetic acid–*N*-methylurea complex with double system of homo- and heteronuclear O–H···O/N–H···O hydrogen bonds: X-ray investigation, ab initio and DFT studies

Agnieszka J. Rybarczyk-Pirek

Received: 22 November 2011 / Accepted: 14 February 2012 / Published online: 9 March 2012
© The Author(s) 2012. This article is published with open access at Springerlink.com

Abstract The X-ray diffraction studies revealed disorder of a trichloroacetic acid–*N*-methylurea complex crystal structure, connected with a proton transfer via O–H···O hydrogen bond. The observed structure corresponds to a co-existence of ionic (salt) and neutral (co-crystal) forms of the complex in the solid state in ratio 3:1, respectively. The geometrical analysis based on ab initio and density functional theory methods combined with the experimental research indicated that two different *N*-methylurea molecular conformations, defined by CNCN torsion angle, correspond to the neutral and the ionic form of the complex, respectively. The conformational changes seem to be connected with stabilization of the ionic structure after a proton transfer, as according to theoretical calculations this form of the complex (the ionic one) was unstable in the gas phase. A particular attention was focused on a system of a double intermolecular hydrogen bonds, O–H···O and N–H···O which join molecules into the title complex. The analysis of these interactions performed in terms of their geometry, energetic and topological electron density properties let for their classification into strong and medium strength hydrogen bonds. It was also found that the antibonding hydrogen bonding donor orbital occupation corresponded to the stabilization energy resulting from charge transfer in hydrogen bonds. Hence, it is postulated as a possible indicator of interaction strength.

Keywords Co-crystal · Hydrogen bonding · Proton transfer · X-ray diffraction · Quantum-chemical calculations · QTAIM

Introduction

Non-covalent interactions have received much interest due to their importance in stabilizing of the molecular arrangement crystal structure in the solid state [1–3]. They range from strong ones, as conventional hydrogen bonds, to weaker as for example van der Waals interactions. Among them the hydrogen bonds are the most favorite and useful in view of their high energy and directionality [4, 5].

Many researches are devoted to very strong hydrogen bonds, because of their important role as a transition state in biochemical reactions and enzyme catalysis [6–12]. Their unusual stabilization energy makes them to be distinguished from ordinary hydrogen bonds. All cases of strong and very strong hydrogen bonds have been classified into charge assisted hydrogen bond (CAHB) and resonance assisted hydrogen bond (RAHB) [13] which have been widely studied [14–23]. The enhancement of hydrogen bonding energy by additional factors, as the polarity of the donor and acceptor groups, can lead to proton transfer between molecules with formation of a salt. In order to convert a neutral hydrogen bond D–H···A into a corresponding ionic one D^{-}···H–A^{+}, external electric field may be required [24–27]. It can be produced by solvent dipoles or the assembly of many hydrogen bond bridges of the same type for example in crystal structure. Proton transfer enables charge and energy transfer in solid chemical and biological systems, thus a degree of cooperativity between these processes occurs.

The further insight into the nature of many types of hydrogen bonds, can be achieved by designing and studying

Electronic supplementary material The online version of this article (doi:10.1007/s11224-012-9980-7) contains supplementary material, which is available to authorized users.

A. J. Rybarczyk-Pirek (✉)
Department of Structural Chemistry and Crystallography, University of Łódź, ul. Pomorska 163/165, 90-236 Lodz, Poland
e-mail: agnesr@uni.lodz.pl

solid state structures of desirable architecture. These processes very often take advantages of mixing different compounds in a one crystal structure: lattice adducts, host–guest compounds, hydrates or solvates, and co-crystals. No doubt that crystalline structure formed of more than one component is thermodynamically stable due to different intermolecular interactions. As a crystal structure is maintained by the whole range of intermolecular interactions the ability of certain functional groups to self-interact in a non-covalent fashion and to retain a specific and persistent patterns, termed as supramolecular synthons [28, 29] is in interest. Among the functional groups used most frequently in crystal engineering is a carboxyl group and its derivatives in relation to amine derivatives. On supramolecular chemistry basis proton donors (organic acid) and acceptors (organic bases) are promising agents to generate stable multi-component hydrogen bonded systems with possible proton transfer via salt bridge [30–34].

Against this background, herein, the results of a co-crystallization trichloroacetic acid with *N*-methylurea are presented. The aim of the presented study was to obtain a new co-crystal structure by using relatively simple molecular building blocks, and to study structural changes within molecular components in relation to intermolecular interactions.

There are known many acid–urea multicomponent crystal structures among them are neutral complexes and ionic structures as well [35–42]. Moreover, the urea is of interest in experimental and theoretical investigations because of simplicity of its molecule [43–46], interesting highly symmetrical crystal structure [47, 48] or physical properties [49, 50]. In contrast, *N*-methylurea co-crystals are little recognized by X-ray methods and up to now only two co-crystal structures have been determined [51, 52]. A change of an urea molecular structure by a simple *N*-methyl substituent disturbs its intrinsic symmetry and gives rise to obtaining novel co-crystal structures governed by wide range of intermolecular interactions. Molecular structure in the solid state compared with a gas phase one obtained from quantum-chemical methods may be a source of information about these interactions in the crystal space [53, 54]. For these reasons a part of this study was focused on theoretical ab initio and density functional theory (DFT) calculations which are combined with X-ray results. The *Atom in Molecules* (QTAIM) and *Natural Bond Orbital* (NBO) theories were utilized to obtain information about interactions in a region of intermolecular bonding.

Experimental

Preparation of crystals

Crystal suitable for X-ray measurement were obtained from commercially available reagents: trichloroacetic acid (**tcla**) and *N*-methylurea (**nmur**) (Aldrich Chemical Company), which were used without further purification.

1 mmol (0.0741 g) of *N*-methylurea were added to three different solvents: methanol, ethanol, and isopropyl alcohols. The solutions were mixed and gently warmed up to temperature up to 50 °C until dissolvation. Then, trichloroacetic acid was added in excess of 1:1 molar ratio. The solutions were again mixed and after the added reagent was dissolved they were stayed in room temperature for several days to obtain crystals by slow evaporation of solvent. Crystals suitable for X-ray diffraction were selected from ethanol solution (Scheme 1).

X-ray structure determination and refinement

A representative crystal of a suitable size was selected and mounted on a fiber loop and used for X-ray measurements. X-ray data were collected at low temperature on a Gemini A Ultra diffractometer equipped with Mo Kα X-ray source and a graphite monochromator. Accurate unit cell parameters were determined using the program CrysAlis CCD [55]. A face-indexed analytical absorption correction was applied. The crystal structure was solved in $P2_1/c$ space group by direct methods using SHELXS-86 [56] and refined by full-matrix least square method using SHELXL-97 [57] (both programs implemented in WinGX [58]). All non-hydrogen atoms were refined with anisotropic displacement parameters. Hydrogen atoms of a methyl group were introduced in calculated positions with idealized geometry (HFIX 137) and refined using a rigid body model. Amine and hydroxyl hydrogen atom positions were located on difference Fourier map. Detailed analysis of this

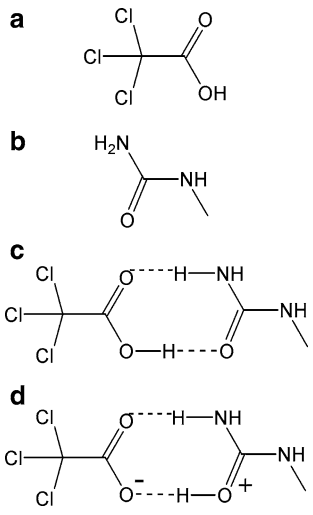

Scheme 1 Structural diagrams: **a** trichloroacetic acid (**tcla**); **b** *N*-methylurea (**nmur**); **c** neutral structure of hydrogen bonded trichloroacetic acid–*N*-methylurea complex; **d** ionic structure of hydrogen bonded trichloroacetic acid–*N*-methylurea complex (salt)

Table 1 Crystallographic data and structure refinement details

Crystal data	
Formula (salt form)	$[C_2H_7N_2]^+[C_2Cl_3O_2]^-$
Formula weight	237.47
Crystal system, space group	Monoclinic, $P2_1/c$
Unit cell dimensions	$a = 8.9759(1)$ Å
	$b = 11.4516(2)$ Å
	$c = 11.9249(3)$ Å
	$\beta = 131.027(1)°$
V	924.70(3) Å^3
Z, d_x	4, 1.706 g/cm^3
Absorption coefficient	0.961 mm^{-1}
$F(000)$	480
Crystal size	0.47 × 0.40 × 0.29 mm
Data collection	
Temperature	100 K
Radiation type, wavelength	Mo Kα, 0.71073 Å
θ range for data collection	2.88–25.00°
Limiting indices	$-10 \le h \le 8$
	$0 \le k \le 13$
	$0 \le l \le 14$
Reflections collected/unique	1633/1633 [$R_{(int)} = 0.022$]
Completeness	99.8%
Refinement	
Refinement method	Full-matrix least-squares on F^2
Data/restraints/parameters	1633/0/113
Goodness-of-fit on F^2	1.135
Final R indices [$I > 2\sigma(I)$]	$R_1 = 0.0194$, $wR_2 = 0.0491$
R indices (all data)	$R_1 = 0.0197$, $wR_2 = 0.0493$
Largest diff. peak and hole	0.314 and −0.284 e/Å^3

map let conclude of proton position disorder within an intermolecular hydrogen bond. The crystal structure was refined as a disordered one with the occupancy factors equal 0.75 for the major component of disorder (salt structure) and 0.25 for the minor one (co-crystal structure). In the final step of refinement procedure, atoms taking part in hydrogen bonds were refined by using some restrains (AFIX 93 and 43 for NH_2 and NH groups, respectively, and AFIX 147 for a hydroxyl group).

The molecular geometry was calculated by PARST [59] and Platon [60]. Selected bond distances and angles summarized in Table 2. Mercury version 1.2.1[1] was used to view hydrogen bond network. A summary of crystallographic relevant data is given in Table 1. As the major component disorder represents a salt—such a formula is given in the table.

[1] Cambridge Crystallographic Data Centre, 12, Union Road, Cambridge CB2 1EZ, UK; fax: +44 1223 336033.

Atoms' coordinates and displacement parameters are deposited with Cambridge Crystallographic Data Centre. CCDC 849679 number contains the supplementary crystallographic data for this article. These data can be obtained free of charge via http://www.ccdc.cam.ac.uk/conts/retrieving.html (or from Footnote 1).

Computations

Quantum-chemical calculations were performed to study the structure and stability of the title complex. The starting geometrical parameters of the complex were taken directly from X-ray analysis. Single molecules and ions of trichloroacetic acid and *N*-methylurea resulting from proton transfer were also considered. All the theoretical calculations were performed with the Gaussian 03 sets of codes [61]. Molecular geometries and their electronic wave function have been optimized with second-order Møller–Plesset perturbation theory (MP2) and DFT methods with B3LYP functional, atomic basis sets 6-311++G(d,p) and aug-cc-pVDZ were utilized. In order to insure adequate convergence, the cutoffs on forces and step size that are used to determine convergence were tightened in calculations. Stationary points corresponding to local energy minima were identified by the absence of imaginary frequencies. For a comparison, single point calculations were also performed for structure determined by X-ray method with the use of the mentioned methods and basis sets.

The Quantum Theory of "Atoms in Molecules" (QTAIM) [62] was applied for ab initio and DFT results to get insight in the nature of interatomic bonds in the investigated systems. The calculations were carried out with AIM2000 program [63] and AIMAll package [64] to find and characterize bond critical points (BCPs).

The Natural Bond Orbital method (NBO program, implemented in Gaussian-03 package) [65] was employed to study charge transfer energy associated with the intermolecular interactions.

Discussion

The structure of the complex in the crystal state

The title complex crystallizes in a centrosymmetric monoclinic space group $P2_1/c$ with one trichloroacetic acid molecule and one *N*-methylurea molecule in the asymmetric unit forming acid–base 1:1 complex (Fig. 1). The molecules are connected into a complex by a double hydrogen bond system involving O1···O3 and O2···N2 interactions.

The step of proton location on a difference Fourier map revealed that the title complex is in an ionic form with one

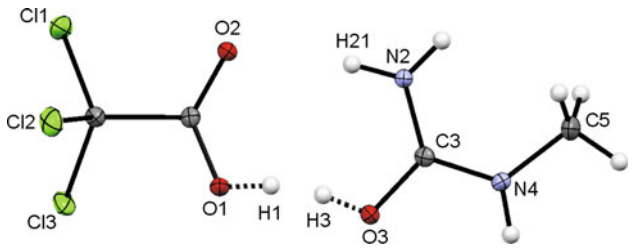

Fig. 1 Molecular drawing of trichloroacetic acid–*N*-methylurea complex as determined by X-ray analysis. Atomic displacement ellipsoids are drawn at the 30% probability level. Covalent bonds to hydrogen atom of a disordered position are presented with *dotted lines*

H atom transferred from acid molecule (O1 atom) to the carbonyl group (O3 atom) of the *N*-methylurea moiety. The map shows two electron density maxima corresponding to positions of hydrogen atoms in neighborhood of O3 and N2 atoms (Fig. 2a). The further analysis of the Fourier map indicated another one electron density maximum (Fig. 2b). This observation gave evidence of the partial presence, a neutral form with a hydrogen atom retained to the carboxyl group. It was also confirmed by relatively short C1–O1 distance of 1.255 Å in comparison with typical C–O(H) bond length of carboxylic acids—1.308 Å [66]. Together these data indicate that the hydrogen atom is shared between O1 and O3 atoms over two position resulting in ionic and neutral form simultaneously with the distribution ratio 3:1, respectively.

In case of ionic structure of complex some degree of charge delocalization is expected. Redistribution of negative charge within the carboxylate group should lead to equalization of C–O bonds. Even though the trichloroacetic anion seem to be almost symmetric (with C_s symmetry plane passing through Cl1, C2 and C1 atoms) it is in the asymmetric environment in the space (compare hydrogen bonding scheme in Fig. 3). As the intermolecular forces break down its intrinsic symmetry it manifests itself by differentiation of bond lengths. The observed shortening of C1–O1 bond length in the carboxylate group bond corresponds to a delocalized double bonds in carboxylate anions (1.254 Å) [66]. However, C1–O1 and C1–O2 bonds are not equal (Table 2). First, one of them cannot be treated as fully deprotonated (partial proton and charge transfer resulting from crystal structure disorder), second, both oxygen atoms take part within the investigated complex as acceptors of different hydrogen bonding type—homonuclear O–H···O1 and heteronuclear N–H···O2.

Another observation of the trichloroacetic anion is differentiation of three C–Cl covalent length bonds. C2–Cl1 is evidently shorter than C2–Cl1 and C2–Cl3, which is in relation with its close position to the carboxylate plane (standard deviation of Cl1 atom from the O1, O2, C1 least

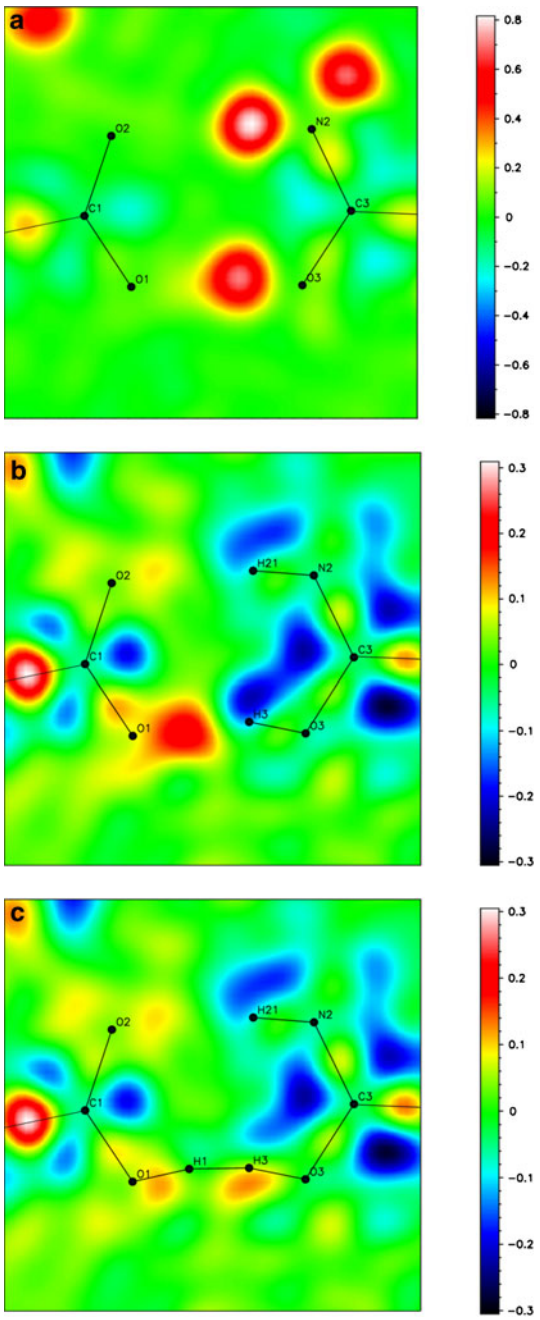

Fig. 2 Difference Fourier maps in the region of O–H···O and N–H···O hydrogen bonding between trichloroacetic acid and *N*-methylurea molecules. The *color code* is shown by the *color bar* in e/Å^3: **a** map calculated for a model without hydrogen atoms positions; **b** map calculated for a model containing hydrogen atoms positions (*ordered structure*); **c** map calculated for a model containing disordered hydrogen atoms positions (*disordered structure*) (Color figure online)

square plane is 0.494(1) Å with corresponding Cl1–C2–C1–O1 torsion angle equal to 162.5(1)°).

Formation of a ionic structure results in distribution of positive charge within cation molecule. As a result *N*-methylurea of protonation C3–O3 bond (1.304(2) Å) is

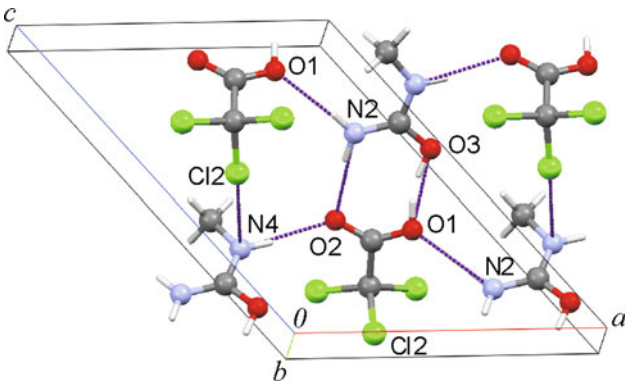

Fig. 3 Scheme of molecular packing and intermolecular interactions (drawn with *dotted lines*) in the crystal structure. There are hydrogen and halogen bonds presented in the figure

longer than typical double C=O bond in urea (1.258 Å) [43] or its derivatives (1.256 Å) [66]. It corresponds well to C–O(H) bond length in urea and *N*-methylurea derivatives reported as ionized structures [38, 51, 67–69] with CO bond lengths in range of 1.29–1.31 Å. Because of evident shortening in comparison with formally single bond, as for example in enol molecules (1.330 Å) it should be considered as an intermediate between a single and a double one.

Both C–N bonds are very short and equal with each other within 3σ criterion. With the bond lengths of 1.316(2) and 1.319(2) Å, they are evidently shorter than in a neutral urea molecule (1.343 Å) [43] or other N-substituted urea derivatives (1.363 Å) [66]. Typical single CN bonds are reported as about 1.33–1.35 Å long with average value 1.346 Å observed for amides. In turn, double CN bonds are in range of 1.28–1.30 Å. The observed large CN bonds shortening is caused not only by electron delocalization but also probably by molecule protonation. It should be noted that for other urea and *N*-methylurea protonated structures the same CN bonds shortening is reported [38]. The observed character of covalent CO and CN bonds indicates that electron and formal positive charge delocalization involves mainly NCN atoms of **nmur**. Planar arrangement of C3, O3, N2, and N4 atoms (the maximum deviation for the least square plane equals 0.06(2) for C3 atom) is another evidence of the postulated electron delocalization.

The crystal structure demonstrates the maximized hydrogen bond interactions with all the potential donors and acceptors utilized. A resulting infinite three-dimensional network is displayed in the packing diagram (Fig. 3). The graph–set analysis let distinguish four different first level motifs of the dimeric type [28], all

Table 2 Selected geometric parameters retained from experiment in comparison with MP2/6-311++G(d,p) (left) and B3LYP/aug-cc-pVDZ (right) calculations (Å, °)

	Crystal structure	Neutral complex (optimized structure)	Neutral monomer (optimized structure)	Ionic monomer (optimized structure)
Cl1–C2	1.759(1)	1.761/1.785	1.757/1.780	1.783/1.819
Cl2–C2	1.781(1)	1.778/1.803	1.775/1.802	1.794/1.828
Cl3–C2	1.768(1)	1.773/1.803	1.775/1.802	1.792/1.827
O1–C1	1.255(2)	1.307/1.304	1.341/1.342	1.241/1.239
O2–C1	1.233(2)	1.216/1.218	1.203/1.201	1.240/1.238
C1–C2	1.566(2)	1.553/1.564	1.548/1.556	1.628/1.641
O3–C3	1.304(2)	1.244/1.254	1.223/1.228	1.318/1.322
N2–C3	1.319(2)	1.365/1.354	1.393/1.378	1.332/1.322
N4–C3	1.316(2)	1.365/1.362	1.378/1.376	1.314/1.319
O2–C1–O1	128.00(1)	127.38/127.37	125.48/125.26	134.12/134.43
O2–C1–C2	118.04(1)	121.89/120.98	124.70/124.00	114.59/114.11
O1–C1–C2	113.93(1)	110.72/111.65	109.81/110.74	111.29/111.46
C1–C2–Cl1	112.31(9)	110.22/110.98	109.61/110.23	113.54/114.36
C1–C2–Cl2	106.52(9)	107.37/108.79	108.08/108.67	108.72/109.91
C1–C2–Cl3	110.43(9)	108.93/108.74	108.10/108.68	109.48/110.16
C3–N4–C5	124.5(1)	123.99/124.55	124.84/125.98	124.55/125.01
O3–C3–N4	115.5(1)	120.28/115.54	122.55/119.44	115.54/115.17
O3–C3–N2	121.6(1)	122.93/121.77	122.56/122.49	121.77/122.03
N4–C3–N2	122.7(1)	116.77/124.55	114.71/118.08	124.55/122.81
Cl1–C2–C1–O1	−162.5(1)	−175.6/178.0	−179.9/−178.0	−177.1/−179.1
C5–N4–C3–N2	6.1(2)	−14.4/0.1	−14.9/10.3	6.6/0.2
C5–N4–C3–O3	−175.1(1)	164.0/−180.0	169.9/−168.3	−173.8/−179.8

Table 3 Hydrogen (D–H···A) and halogen (D–X···A) bonding geometry in the crystal structure

D–H/X···A	*d*(D–H)	*d*(H···A)	*d*(D···A)	∠D–H···A
O1–H1···O3[a]	0.84	1.69	2.506(1)	162.2(1)
O3–H3···O1[b]	0.84	1.70	2.506(1)	161.3(1)
N2–H21···O2	0.88	2.05	2.925(1)	170.5(1)
N2–H22···O1[i]	0.88	2.15	2.994(2)	161.6(1)
N4–H41···O2[ii]	0.88	2.00	2.866(2)	167.6(1)
C2–Cl2···N4[iii]	1.781(1)	3.193(2)	4.939(2)	165.9(1)

Symmetry codes: (i) x, $1/2 - y$, $1/2 + z$, $-z$; (ii) $1 + x$, $1/2 - y$, $1/2 + z$; (iii) $-1 + x$, y, $-1 + z$

[a] Hydrogen bond corresponding to neutral (co-crystal) structure

[b] Hydrogen bond corresponding to ionic (salt) structure

between neighboring **tcla** and **nmur** molecules. Three of them are heteronuclear hydrogen bonds of the type N–H···O. The remaining O–H···O interaction is related to the mentioned proton transfer. The geometric parameters of hydrogen bonding are given in Table 3.

The graph set analysis reveals interesting features of the hydrogen bonds at the second level network. As a result of the hydrogen bonding a ring motif $R_2^2(8)$ within complex is formed. But when considering hydrogen bonds outside the complex a chain motif $C_2^2(8)$ along crystallographic a axis can be distinguished. Although there are similarities in the N–H···O interactions within this chain, their geometries are different as it is given in the Table 4. Analysis of other intermolecular distances revealed the existence of a short Cl2···N4 contact that should be treated as a halogen bonding. Such an interaction seems to be a factor responsible for the C–Cl2 bond elongation in comparison with C–Cl3.

When considering major component of disorder the resulting structure may be regarded as an acid–base complex linked by a double system of (+/−) charge assisted hydrogen bonds ((+/−)-CAHB).

The gas phase theoretical calculations: comparison of molecular geometry

The first step of computations was connected with the stability of the title complex in its both ionic and neutral forms, as an isolated structure. As a starting point the geometry of ionic form (the major crystal disorder component) was taken. The optimizations were made with the use of two different methods (MP2 and B3LYP) with 6-311++G(d,p) basis set utilized. In both methods as a results of molecular optimization the initial ionic structure collapsed without activation barrier to a neutral complex form. In case of DFT calculation method some imaginary frequencies occurred indicating that final stationary point corresponds to a transition state. These frequencies were

Table 4 Topological parameters of hydrogen bonding from QTAIM topological analysis; MP2/6-311++G(d,p) results

Bond	ρ_{BCP}	$\nabla^2\rho_{BCP}$	V_{BCP}	H_{BCP}
Salt (single point calculations for the crystal structure)				
O3–H3···O1				
H3···O1	0.064	0.150	−0.066	−0.014
O3–H3	0.340	−2.446	−0.767	−0.689
N2–H21···O2				
H21···O2	0.029	0.085	−0.021	0.000
N2–H21	0.311	−1.704	−0.512	−0.469
Co-crystal (single point calculations for the crystal structure)				
O1–H1···O3				
H1···O3	0.068	0.178	−0.079	−0.017
O1–H1	0.300	−2.231	−0.680	−0.619
N2–H21···O2				
H21···O2	0.026	0.101	−0.021	0.002
N2–H21	0.317	−1.894	−0.548	−0.511
Neutral complex (optimized structure)				
O1–H1···O3				
H1···O3	0.063	0.156	−0.067	−0.014
O1–H1	0.303	−2.049	−0.645	−0.579
N2–H21···O2				
H21···O2	0.025	0.092	−0.018	0.002
N2–H21	0.330	−1.719	−0.527	−0.478

In the table are presented: electron density (ρ_{BCP}), Laplacian of electron density ($\nabla^2\rho_{BCP}$), potential (V_{BCP}) and total energy density (H_{BCP}) in BCPs (a.u.)

connected with unstable structure of **nmur** due to inversion of pyramidal geometry around N atoms, and with rotation of trichloromethyl group around CC bond of **tcla** molecule. For further comparison additional B3LYP calculations were made with the use of aug-cc-pVDZ basis set also leading to the final neutral complex form. Consequently, the results of MP2/6-311++G(d,p) and B3LYP/aug-cc-pVDZ calculations, which led to local energy minimum stationary points, were taken for further geometrical analysis.

The geometric parameters calculated for crystal, optimized geometry complex and single molecules of trichloroacetic acid and *N*-methylurea, in theirs ionic and neutral forms, presented in Table 2 show some discrepancies concerning conformations and bond lengths of ionic and neutral form.

For ideal C_s symmetry of trichloroacetic acid anion a mirror plane should pass through the carboxylate group, the C1 and C2 carbon atoms and one of the chlorine atoms with Cl1–C2–C1–O1 torsion angle equal 180°. In theoretical calculations **tcla** conformation defined by ClCCO torsion angle is much closer to C_s symmetry, than in the crystal structure. This difference is caused by Cl2···N4

halogen bonding which stops rotation of trichloromethyl group along C1–C2 bond in the crystal. For B3LYP method, the structure of the **tcla** molecule is very close to C_s symmetry for all the investigated species. In case of MP2 computations, even though starting from the same crystal geometry, this symmetry is not retained especially for the optimized complex and the ionic form of monomer, which much more resemble the situation in the crystal, indicating that ionization, connected with hydrogen bond formation and proton transfer, is a process accompanied by breaking down C_s symmetry.

Within trichloroacetic acid molecule C2–Cl1 bond is always the shortest of C–Cl bonds, which is accompanied by increase of respective C1–C2–Cl1 valence angle. This shortening is the same magnitude for the all the optimized species—the complex and the both monomeric forms and it is not connected with hydrogen bonding formation in the crystal structure. On the base of the theoretical computations the other two C–Cl bonds do not differ in length, as it is observed in the crystal structure with bond lengths differentiation of 0.013(1) Å due to the mentioned halogen bonding. C–O carboxylate bonds lengths in the crystal structure quite well correspond to the ionic structure with some degree of their length differentiation. In turn, the valence angle O1–C1–O2 in crystal structure is larger than 120° and of middle value between the neutral and the ionic structure. The gas-phase calculations give very large elongation of the ionic C1–C2 in trichloroacetic acid molecule, especially in the B3LYP level of calculation, which does not take place in the solid state.

For an ideal C_s symmetry of *N*-methylurea a mirror plane should pass through all the non-hydrogen atoms with torsion angle C5–N4–C3–N2 equal to 0°. Such planar symmetry is not observed in the investigated crystal structure. In general also theoretical calculations give a non-planar arrangement of CNCN atoms with corresponding torsion angle larger than 10° (both methods except of the structure of complex obtained from DFT) indicating pyramidal geometry of the N3 atom (Table 2). While comparing the optimized geometry structures with the X-ray observations, again MP2 results for the ionic **nmur** monomer are in better agreement with the experiment than B3LYP.

The most meaningful differences in *N*-methylurea geometry are observed around C3 atom. First, the C3–O3 bond in the crystal structure is elongated as a result of ionization but not as far as for the both calculated ionic forms. The geometrical parameters also does not show the equalization of C3–N bonds for the theoretical gas-phase structure even though it is observed in the crystal. Moreover, C3–N2 and C3–N4 bonds are evidently shorter from experimental X-ray studies than from theoretical calculations. Again all these differences in bond lengths are accompanied by changes in valence angles around C3 atom.

In summary, conformation of both trichloroacetic acid and *N*-methylurea moieties in the crystal much better corresponds to the conformations obtained from MP2 method performed for the ionic forms than from B3LYP. All the bond lengths and valence angles changes observed in the investigated structure seem to be mainly directed by the ionic salt–neutral complex disorder nature of the presented crystal. MP2 computations also give geometrical evidence that crystal structure represent a "frozen state" of ionic cation–anion structure and this one had to be a dominant one in process of crystal formation and the proton transfer evidenced as the observed proton disorder has to be a secondary process taking place in the crystal after forming solid structure.

Topological analysis of interatomic electron density: QTAIM approach

An analysis of covalent bonding character of the title complex was made from point of view of electron density distribution. Figure 4, presents the structure of the

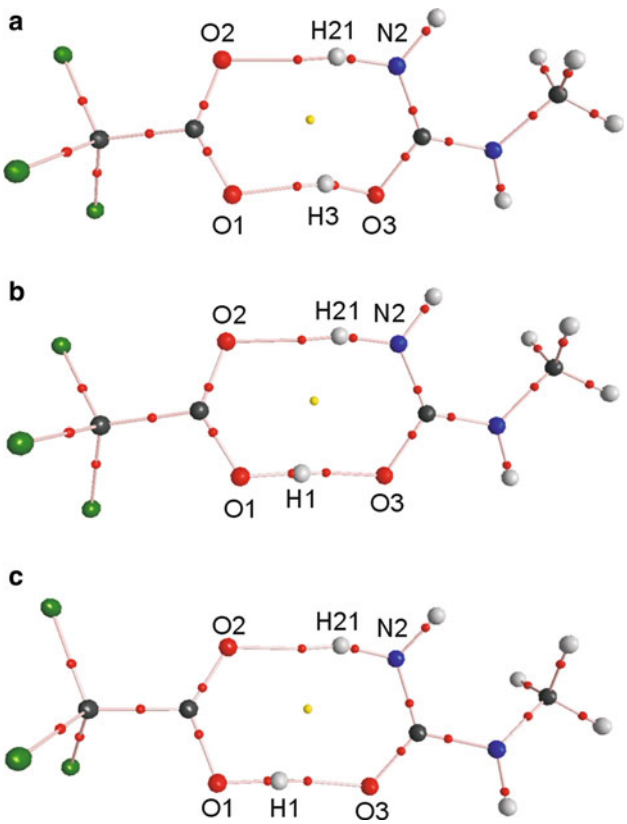

Fig. 4 Molecular graphs as the title complex obtained from QTAIM analysis. *Lines* correspond to bond paths, *red circles* to bonds critical points and *yellow* to ring critical points: **a** single point calculations for a ionic structure (major component of crystal disorder); **b** single point calculations for a neutral complex (minor component of crystal disorder); **c** optimized structure–neutral complex (Color figure online)

investigated complexes with bond paths, nuclear attractors, bond and ring critical points as obtained from MP2 calculations. The QTAIM parameters computed for the crystal structure geometry (single point calculations), the optimized structure of the complex and the corresponding monomers of selected BCP are collected in the supplementary Table S5. Among them the most important is electron density (ρ_{BCP}). Its values for both calculation methods, MP2 and DTF, are in good agreement with no significant differences. Major discrepancies are observed for the Laplacians of the electron density ($\nabla^2\rho_{BCP}$) which suggests the comparison should be rather qualitative. As the Laplacian of the electron density is a very sensitive criterion to detect insufficient description of electronic structure, positive values obtained for C1–O2 bond in optimized structures (B3LYP/aug-cc-pVDZ) suggest inadequate level of theory employed, so the further topological electron density analysis is based on MP2 results. For all the covalent bonds Laplacians are negative with the lowest values of N–C bonds (−1.1 to −0.9 a.u.) indicating large concentration of the electron density. Comparatively, C–O bonds in **tcla** moiety even when considered as formally double ones, have higher values of $\nabla^2\rho_{BCP}$ in range of −0.2 to −0.5 a.u. When comparing Laplacians of all the investigated species the largest inconsistencies are observed for the single point neutral complex based on the crystal structure geometry which again confirms that crystal much more resembles cation–anion salt structure than a co-crystal one.

As a measure of non-spherical charge distribution in BCP ellipticity ε_{BCP}, is a source of information about π-bond character. C1–C2 and N4–C5 as formal single bonds have small values of ellipticity comparable to known literature [70–72]. N–C3 in **nmur** moiety may be considered as double ones with ε_{BCP} about 0.2. For C–O bonds ellipticity is evidently smaller and decreases to 0.01 for C1–O1 single bond and up to 0.09 for C1–O2 double bond in a monomer. In the investigated complexes these two bonds as well as C3–O3 should be described as intermediate between single and double, which is reflected by medium ranges of their ellipticities. As the changes of bond ellipticities are in agreement with the observations of bond lengths changes the latter are attributed to π-delocalization effects.

An insight into nature of intermolecular interactions

The topology of the electron density at BCP is an indicator of the strength of intermolecular interactions [73, 74]. Table 4 (Table S6 in supplementary materials for both computational methods) presents selected topological parameters of hydrogen BCPs. The differences between characteristics of BCPs for the ionic and the neutral complexes, as obtained from the single point calculation of crystal geometry structures and for the optimized species, are meaningless. As the electron density at proton-acceptor hydrogen bonds correlates with hydrogen bond energy [74] O–H···O hydrogen bond with relatively large electron densities (0.063–0.072 a.u.), are much stronger than N–H···O (ρ_{BCP} in range 0.025–0.029 a.u.) in all the investigated structures. It supports the geometrical findings as O–H···O intermolecular contacts are evidently shorter than and N–H···O (Table 3).

Further topological parameters at hydrogen bonds critical points are close to each other for all the investigated species. Some discrepancies are observed for O–H···O hydrogen bond in the crystal geometry single point neutral structure, where Laplacians of electron density ($\nabla^2\rho_{BC}$), the kinetic electron energy densities (G_{BCP}), and the potential electron energy density (V_{BCP}) have little higher values in comparison with the single point ionic crystal structure and the optimized neutral complex. The presented values of H_{BCP}, corresponding to proton–proton acceptor interaction, indicate that all the O–H···O bonds are strong of the partially covalent nature hydrogen bonds [74], while N–H···O should be classified as medium strength ones. As the existence of strong hydrogen bonds enables proton transfer the evidence of such a phenomenon is observed in the investigated structure and consequently, there are also no observations of proton transfer via weaker heteronuclear N–H···O bond.

Formation of a hydrogen bond implies that a certain amount of electronic charge is transferred from the proton acceptor to the proton donor molecule. The role of this charge transfer can be carried out by considering interactions between filled acceptor lone pairs and empty donor orbitals and estimation their energetic importance by second-order perturbation theory according to Natural Bond Orbital Theory (NBO). For the investigated structures, NBO orbital interaction energies together with the overall transferred charge (CT) from one molecule to the other they are summarized in Table 5 for MP2 optimized geometry and in supplementary material (Table S5) for both computational methods. The main complex stabilization energy arises from the electronic charge transfer from the lone pairs of proton acceptor to antibond H-Donor sigma orbitals and there is a good agreement between results calculated for the single point co-crystal geometry and the optimized neutral complex, than in case of the ionic crystal structure.

As expected the largest charge transfer is observed for the ionic–salt structure, but it differs from unity indicating the additional charge transfer from trichloroacetic acid anion to *N*-methylurea cation via system of double hydrogen bonds. This additional charge transfer amounts about 0.16e and mainly comes from lone pair to

Table 5 NBO analysis of hydrogen bonds based on MP2/6-311++G(d,p) optimized geometry

Bond	Orbital interaction	$E(2)$	ΔLP	ΔBD*	CT
Salt (single point calculations for the crystal structure)					
O3–H3···O1	LP(1)O1 → BD*(1)O3–H3	6.36	16.78	−92.06	846.15
	LP(2)O1 → BD*(1)O3–H3	34.51	39.34		
N2–H21···O2	LP(1)O2 → BD*(1)N2–H21	3.31	9.50	−45.05	
	LP(2)O2 → BD*(1)N2–H21	12.72	11.00		
Co-crystal (single point calculations for the crystal structure)					
O1–H1···O3	LP(1)O3 → BD*(1)O1–H1	8.60	17.90	−75.50	61.82
	LP(2)O3 → BD*(1)O1–H1	55.44	17.76		
N2–H21···O2	LP(1)O2 → BD*(1)N2–H21	4.25	6.31	−19.39	
	LP(2)O2 → BD*(1)N2–H21	10.29	7.71		
Neutral complex (optimized structure)					
O1–H1···O3	LP(1)O3 → BD*(1)O1–H1	11.31	28.79	−82.52	62.96
	LP(2)O3 → BD*(1)O1–H1	34.09	12.29		
N2–H21···O2	LP(1)O2 → BD*(1)N2–H21	3.71	8.27	−21.92	
	LP(2)O2 → BD*(1)N2–H21	6.41	9.89		

Corresponding donor–acceptor natural bond orbital interactions with second-order perturbation stabilization energy $E(2)$ (kcal/mol) are presented. ΔLP, ΔBD* and CT represent consequently: lone pairs and antibonding molecular orbitals relative occupation changes (calculated as a difference between orbital occupancy in free monomer and complex) and overall charge transfer between molecules (me)

antibonding orbital LPO1 → BD*O3–H3 interactions, but is also enhanced by LPO2 → BD*N2–H21 interaction which is reflected by changes in antibonding ΔBD* N2–H21 orbital occupation in comparison with a free *N*-methylurea molecule. On the other side, in case of the both neutral forms (co-crystal single point and complex optimized) the overall intermolecular electronic charge transfer amounts about 0.06e. Here, the main stabilization energy comes from LPO3 → BD*O1–H1 orbital interactions.

Considering all the investigated structures the amounts of the transferred charge is evidently larger for the O–H···O interaction than for the N–H···O one and these differences are consistent with the corresponding interaction energies. A common feature of all the studied complexes is an increase of the electronic charge on antibonding orbital and decrease of it on hydrogen bonds acceptors lone electron pairs in comparison with the corresponding free monomer molecules. The changes of occupation for the interacting antibonding orbitals (ΔBD*) are related to corresponding stabilization energy and consistent with each other. Much more inconsistencies occur for changes in hydrogen bonding acceptors lone pairs occupation (ΔLP), especially for B3LYP optimized geometry. In general, the relation between total interaction energy $E(2)$ and antibonding orbital occupation changes can be directed for all the species investigated, but not for changes of lone pairs occupation. Hence, the change in corresponding antibonding orbital occupation (ΔBD*) seems to be a better indicator of interaction strength than sum of lone pairs occupation changes (ΔLP) for which some inconsistencies depending on calculation method are evident.

Conclusion

The presented study demonstrates the structural complexity of experimental crystallographic and theoretical quantum-chemical methods in the case of trichloroacetic acid–*N*-methylurea complex. The X-ray studies indicated co-existence of two different forms of the two component crystal: the ionic one corresponding to a salt and the neutral one corresponding to co-crystal structure, respectively. This phenomenon was attributed to the proton transfer via system of double O–H···O/N–H···O hydrogen bonds.

In the investigated case, quantum theoretical MP2/6-311++G(d,p) method become more useful tool for studying structural changes connected with proton transfer than B3LYP/aug-cc-pVDZ as it much better resembles geometrical features of the crystal. It also lead to electron density topological analysis results in better agreement with experiment.

The theoretical computations indicated that the neutral form of the complex is stable in a gas phase, while in the crystal the ionic is a dominating one with stability assured by system of intermolecular interactions of the type hydrogen and halogen bonds. The performed calculations let also find two different molecular conformations of *N*-methylurea moiety: one for the neutral form (*N*-methylurea molecule) and the other one for the ionic form

(*N*-methylurea cation), respectively. The latter corresponded to the determined crystal structure, suggesting that the process of crystallization was based on ionic form of complex.

The topological electron density distribution analysis of BCPs let classify homonuclear O–H···O hydrogen bonds as strong and heteronuclear N–H···O as medium strength ones, which is in agreement with the observed proton transfer. NBO studies based on quantum-chemical calculations confirmed that the main contribution of stabilization energy results from charge transfer between lone O electron pair and antibonding O–H orbital. It also corresponds with the changes of the antibonding donor orbital occupation, which revealed to be a good indicator of interaction strength.

Acknowledgments This study was financially supported by the Grant No. 505/721/R (University of Łódź). Use of Computational resources of the Cracow Supercomputing Centre is acknowledged. Author is grateful to Dr. Magdalena Małecka and Dr. Lilianna Chęcińska from University of Łódź for helpful assistance and to Dr. Olivier Presly from Oxford Diffraction Laboratory for X-ray measurements.

Open Access This article is distributed under the terms of the Creative Commons Attribution License which permits any use, distribution, and reproduction in any medium, provided the original author(s) and the source are credited.

References

1. Desiraju GR (2008) Crystal engineering, the design of organic solids. Elsevier, Amsterdam
2. Braga D, Grepioni F, Desiraju GR (1998) Chem Rev 98:1375–1406
3. Moulton B, Zaworotko MJ (2001) Chem Rev 101:1629–1658
4. Desiraju GR (2002) Acc Chem Res 35:565–573
5. Jeffery GA, Saenger W (1991) Hydrogen bonding in biological structures. Springer, Berlin
6. Cleland WW, Kreevoy MM (1994) Science 264:1887–1980
7. Hur O, Leja C, Dunn M (1996) Biochemistry 35:7378–7386
8. Wu ZR, Ebrahimian S, Zawrotny ME, Thornburg LD, Perez-Alvarado GC, Brothers P, Pollack RM, Summers MF (1997) Science 276:415–418
9. Remer LC, Jensen JH (2000) J Phys Chem A 104:9266–9275
10. Northrop BD (2001) Acc Chem Res 34:790–797
11. Garcia-Viloca M, Gonzalez-Lafont A, Lluch JM (1997) J Am Chem Soc 119:1081–1086
12. Pan Y, MacAllister MA (1997) J Am Chem Soc 119:11277–11281
13. Gilli G, Gilli P (2000) J Mol Struct 552:1–15
14. Fores M, Scheiner S (1999) Chem Phys 246:65–74
15. Gonzalez L, Mo O, Yanez M (1999) J Org Chem 64:2314–2321
16. Król-Starzomska I, Filarowski A, Rospenk M, Koll A (2004) J Phys Chem A 108:2131–2138
17. Zgierski MZ, Grabowska A (2000) J Chem Phys 113:7845
18. Palusiak M, Simon S, Sola M (2009) J Org Chem 74:2059–2066
19. Małecka M, Chęcińska L, Rybarczyk-Pirek A, Morgenroth W, Paulmann C (2010) Acta Crystallogr B 66:687–695
20. Rybarczyk-Pirek AJ, Dubis AT, Grabowski SJ, Nawrot-Modranka J (2006) Chem Phys 320:247–258
21. Rybarczyk-Pirek AJ, Grabowski SJ, Małecka M, Nawrot-Modranka J (2002) J Phys Chem A 106:11956–11962
22. Sobczyk L, Grabowski SJ, Krygowski TM (2005) Chem Rev 105:3513–3560
23. Ferretti V, Bertolasi V, Pretto L (2004) New J Chem 28(2004): 646
24. Herbstein FH (2005) Crystalline molecular complexes and compounds. Oxford University Press, Oxford
25. Ramos M, Alkorta I, Elguero J, Golubev NS, Denisov GS, Benedict H, Limbach HH (1997) J Phys Chem A 101:9791–9800
26. Sharif S, Powell DR, Schagen D, Steiner T, Toney MD, Fogle E, Limbach HH (2006) Acta Crystallogr B 62:480–487
27. Golubev NS, Smirnov SN, Tolstoy PM, Sharif S, Toney MD, Denisov GS, Limbach HH (2007) J Mol Struct 884:319–327
28. Bernstein J, Etter MC, MacDonald JC (1990) J Chem Soc Perkin Trans 2:695–698
29. Desiraju GR (1995) Angew Chem Int Ed 107:2311–2327
30. Wilson CC, Goeta AE (2004) Angew Chem Int Ed 43:2095–2099
31. Parkin A, Adams A, Cooper RI, Middlemiss DS, Wilson CC (2007) Acta Crystallogr B 63:303–308
32. Wilson CC (2001) Acta Crystallogr B 57:435–439
33. Klinman JT, Limbach HH, Schowen RL (eds) (2007) Hydrogen transfer reactions. Wiley–VCH, Weinheim
34. Bürgi HB, Dunitz JD (1983) Acc Chem Res 16:153–161
35. Videnova-Adrabińska V, Etter MC (1995) J Chem Crystallogr 25:823–829
36. Smith G, Baldry KE, Byriel KA, Kennard CHL (1997) Aust J Chem 50:727–736
37. Morrison CA, Siddick MM, Camp PJ, Wilson CC (2005) J Am Chem Soc 127:4042–4048
38. Nelyubina YV, Lyssenko KA, Golovanov DG, Antipin MY (2007) CrystEngComm 9:991–996
39. Gryl M, Krawczuk A, Stadnicka K (2008) Acta Crystallogr B 64:623–632
40. Cruz-Cabeza AJ, Day GM, Jones W (2008) Chem Eur J 14:8830–8836
41. Alhalaweh A, George S, Boström D, Velaga SP (2010) Cryst Growth Des 10:4847–4855
42. Gryl M, Krawczuk-Pantula A, Stadnicka K (2011) Acta Crystallogr B 67:144–154
43. Birkedal H, Madsen D, Mathiesen RH, Knudsen K, Weber HP, Pattison P, Scharzenbach D (2004) Acta Crystallogr B 60:371–381
44. Masunov A, Dannenberg JJ (1999) J Phys Chem A 103:178–184
45. Bharatam PV, Moudgil R, Kaur D (2003) J Phys Chem A 107:1627–1634
46. Jayatilaka D, Grimwood D (2004) Acta Crystallogr A 60:111–119
47. Gatti C, Saunders VR, Roetii C (1994) J Chem Phys 101:10686–10696
48. Olejniczak A, Ostrowska K, Katrusiak A (2009) J Phys Chem C 113:15761–15767
49. Dixon AD, Matsuzawa N (1994) J Phys Chem 98:3967–3977
50. Luo SJ, Yang JT, Du WF, Laref A (2011) J Phys Chem A 115: 5192–5200
51. Bryden JH (1957) Acta Crystallogr 10:714
52. Harkema S, Ter Brake JHM, Meutstege HJG (1979) Acta Crystallogr B 35:2087–2093
53. Rybarczyk-Pirek AJ, Zgierski MZ (2001) J Chem Phys 115:9346–9351
54. Chęcińska L, Grabowsky S, Małecka M, Rybarczyk-Pirek AJ, Jóźwiak A, Paulmann C, Luger P (2011) Acta Crystallogr B 67:569–581
55. Oxford Diffraction (2009) Gemini system and CrysAlis software system. Oxford Diffraction Ltd.

56. Sheldrick GM (1986) SHELXS86 program for crystal structure solution. University of Göttingen, Göttingen
57. Sheldrick GM (2008) Acta Crystallogr A 64:112–122
58. Farrugia LJ (1999) J Appl Cryst 32:837–838
59. Nardelli M (1995) J Appl Cryst 28:659
60. Spek AL (2003) J Appl Cryst 36:7–13
61. Frisch MJ et al (2004) Gaussian 03, revision C.02. Gaussian, Inc., Wallingford
62. Bader RF (1990) Atoms in molecules. A quantum theory. Oxford University Press, New York
63. Biegler-König J, Schönbohm D, Bayles D (2001) J Comput Chem 22:545–559
64. Keith TA (2009) AIMAll (version 09.11.29). aim.tkgristmill.com
65. Weinhold F, Landis F (2005) Valency and bonding. A natural bond orbital donor–acceptor perspective. Cambridge University Press, Cambridge
66. Allen FH, Kennard O, Watson DG, Brammer L, Orpen AG, Taylor R (1987) J Chem Soc Perkin Trans 2:S1–S83
67. Wilson CC (2000) Acta Crystallogr B 57:435–439
68. Rodrigues BL, Tellgren R, Fernandes NG (2000) Acta Crystallogr B 57:353–358
69. Henschel D, Hamann T, Moers O, Blaschette A, Jones PG (2002) Z Naturforsch B Chem Sci 57:113–121
70. Kozisek J, Hansen NK, Fuess H (2002) Acta Crystallogr B 58:463–470
71. Scheins S, Messerschmidt M, Luger P (2005) Acta Crystallogr B 61:443–448
72. Małecka M (2010) Struct Chem 21:175–184
73. Rybarczyk-Pirek AJ, Grabowski AJ, Nawrot-Modranka J (2003) J Phys Chem A 107:2939–9232
74. Grabowski SJ (2011) Chem Rev 111:2597–2625